DALTON

The electronic structure of the mixed-valence copper dimer $[Cu_2\{N(CH_2CH_2N{=}CHCH{=}NCH_2CH_2)_3N\}]^{3+}$ ‡

Jacqueline A. Farrar,[a] Roger Grinter,[a] Frank Neese,[b] Jane Nelson[c] and Andrew J. Thomson*,†,[a]

[a] *School of Chemical Sciences, University of East Anglia, Norwich, UK NR4 7TJ*
[b] *Fakultät für Biologie, Universität Konstanz, D-78464 Konstanz, Germany*
[c] *School of Chemistry, Queens University, Belfast, UK BT9 5AG*

Fully delocalised mixed-valence (MV) copper dimers, $\{Cu^{+1.5}, Cu^{+1.5}\}$, have been identified both in proteins and in model complexes. An interpretation of the electronic transitions observed in the low-temperature magnetic circular dichroism and absorption spectra of one such dimer, $[Cu_2L^{imBT}]^{3+}$, where $L^{imBT} = N(CH_2CH_2N{=}CHCH{=}NCH_2CH_2)_3N$, is presented. The spectrum is dominated by transitions within a set of energy levels derived from almost pure copper 3d orbitals of the $[Cu_2]^{3+}$ core. Limited ligand covalency is found. The MV transition energy has been used to elucidate the valence delocalisation energy which is compared with the delocalisation energies in thiolate bridged MV copper dimers. The delocalisation energy of 7100 cm^{-1} is almost entirely due to copper–copper σ overlap at a distance of 2.36 Å and represents a metal–metal bond $(\sigma)^2(\sigma^*)^1$ with bond order 0.5.

Fully delocalised class III mixed-valence[1] (MV) dicopper co-ordination complexes, containing a Cu^ICu^{II} core, are comparatively unusual. However, in the last few years a number of examples have been reported in a variety of chemical and biological environments. These include the bis(μ-thiolato)dicopper electron-transfer centre found in cytochrome c oxidase and nitrous oxide reductase known as Cu_A,[2–4] a model of the Cu_A site, $[Cu_2(L^{iPrdacoS})_2]^+$ [$L^{iPrdacoS} = SCH_2CH_2(N_2C_6H_{12})CH(CH_3)_2^-$], synthesised with a novel tridentate N_2S ligand[5] and an inorganic complex with nitrogen co-ordination only, due to an octaazacryptand macrobicyclic ligand.[6,7]

There is interest in understanding the electronic structures of such dimers, both to shed light on the pathways of electron delocalisation within the dimeric unit and to understand the role that such centres play in long distance electron transfer between redox centres in proteins. This group of compounds provides examples with copper–copper distances varying between 2.9 and 2.38 Å, with and without bridging thiolate ligands. In spite of such differences the valences are fully delocalised in all three cases. Interest has been focused on the relative contribution to the delocalisation energy of direct metal–metal interactions *versus* that of the bridging ligands. A detailed description of the electronic structure of the Cu_A centre has been given based upon the assignment of the absorption, CD and magnetic circular dichroism (MCD) spectra.[4] This has led to the identification of the MV transition between the highly covalent ψ and ψ* copper–thiolate molecular orbitals responsible for electron exchange. In the case of a mixed-valence copper dimer with $3d^93d^{10}$ electronic configuration the analysis is straightforward since the energy separation of the two states is a direct measure of the delocalisation energy.[8–10]

In this paper we extend our analysis to the MV octaazacryptate complexes. We have previously reported the absorption, MCD and resonance-Raman spectra of three related complexes with cryptates of different cap sizes and linker orientation but with similar Cu–Cu bond lengths.[11] An assignment of the electronic spectra based upon transitions within the copper d-orbital manifold which identifies the MV transition and gives an estimate of the delocalisation energy is proposed in this paper. A comparison is then drawn between the values of the delocalisation energies in the different examples of MV dimers containing the Cu^ICu^{II} core.

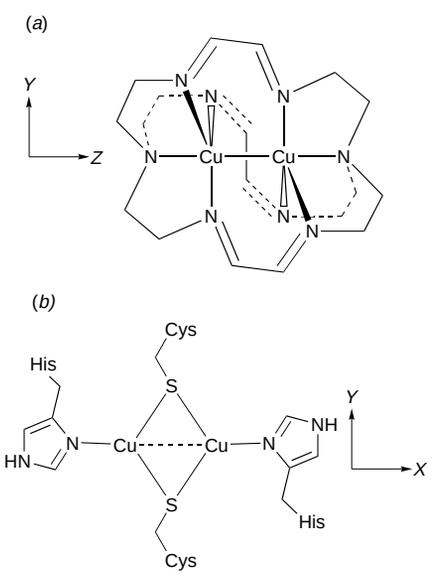

Fig. 1 (*a*) Structure of $[Cu_2L^{imBT}]^{3+}$, showing the axis system used for interpretation of the spectroscopic data. (*b*) Minimal model of the Cu_A centre used to interpret the optical data,[4] in which there are two bridging cysteine (Cys) residues and each copper ion is bonded to a terminal histidine (His) residue

Results and Discussion

The copper dimer of interest in this work, $[Cu_2L^{imBT}]^{3+}$, consists of two copper ions within an azacryptand cage, Fig. 1(*a*), where $L^{imBT} = N(CH_2CH_2N{=}CHCH{=}NCH_2CH_2)_3N$. For comparison, the structure of the Cu_A centre is shown in Fig. 1(*b*). The magnetic properties and optical spectra of the dicopper octaazacryptands can be interpreted by considering a $[Cu_2]^{3+}$ unit which is perturbed by a trigonal ligand field (C_{3v}) around each copper ion. Hence, considering only the first co-ordination sphere, the states of $[Cu_2L^{imBT}]^{3+}$ can be classified under D_{3d} symmetry. Fig. 1(*a*) shows the axis system used, in which the Cu–Cu direction lies along the unique (*Z*) axis. Since the molecule is axially symmetric, orbital angular momentum of the copper 3d orbitals is maintained about the unique axis with

† E-mail: a.thomson@uea.ac.uk
‡ Based on the presentation given at Dalton Discussion No. 2, 2nd–5th September 1997, University of East Anglia, UK.

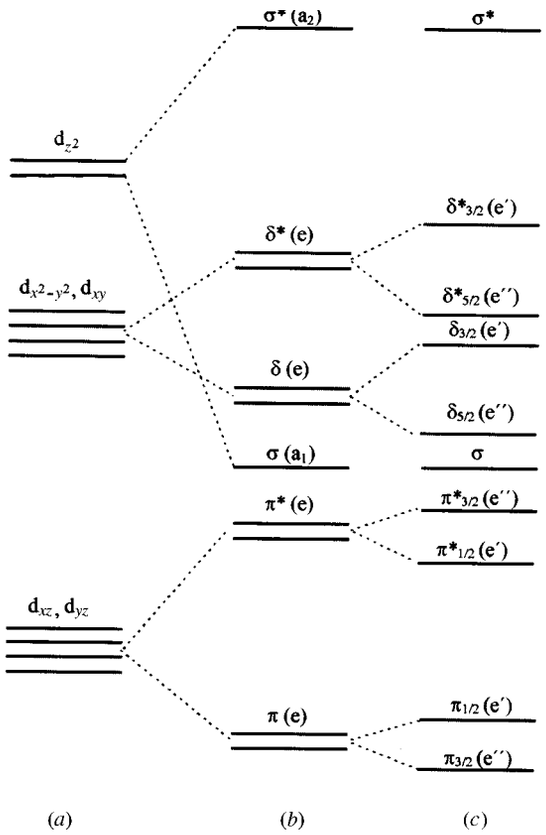

Fig. 2 Proposed energy level diagram of $[Cu_2L^{imBT}]^{3+}$ (*a*) under C_{3v}, (*b*) under D_3 and (*c*) after taking account of the effect of first-order SOC. In (*b*) the orbitals are labelled according to the angular momentum along the *Z* axis and according to the representation under D_3. In (*c*) the orbitals which transform as e are additionally labelled according to the double group representation. The ordering in (*b*) has been confirmed by extended Hückel molecular orbital (EHMO) calculations on a simple H_3N–Cu–$(NH{=}CHCH{=}NH)_3$–Cu–NH_3 model

$M_L = 0, \pm1, \pm2$ to give the following molecular orbitals (MOs) σ (d_z^2) and σ* (d_z^2) with $M_L = 0$, π (d_{xz}, d_{yz}) and π* (d_{xz}, d_{yz}) with $M_L = \pm1$, and δ (d_{xy}, $d_{x^2-y^2}$) and δ* (d_{xy}, $d_{x^2-y^2}$) with $M_L = \pm2$. Hence the orbitals in the energy level scheme given in Fig. 2(*b*) are classified under D_3, see below, and according to the orbital angular momentum about the unique axis. The dimer $[Cu_2]^{3+}$ possesses one unpaired electron and therefore all the electronic states will be doubly degenerate with $S = \frac{1}{2}$. When spin–orbit coupling within, but not between, the states is considered the total angular momentum, M_J, along the *Z* axis is conserved and so the spin–orbit components of each state become $^2\Sigma_0$, $^2\Sigma^*_0$ ($M_J = 0$), $^2\Pi_{\frac{1}{2}}$, $^2\Pi_{\frac{3}{2}}$, $^2\Pi^*_{\frac{1}{2}}$, $^2\Pi^*_{\frac{3}{2}}$ ($M_J = \pm\frac{1}{2}, \pm\frac{3}{2}$), and $^2\Delta_{\frac{3}{2}}$, $^2\Delta_{\frac{5}{2}}$, $^2\Delta^*_{\frac{3}{2}}$, $^2\Delta^*_{\frac{5}{2}}$ ($M_J = \pm\frac{3}{2}, \pm\frac{5}{2}$). Consideration of spin–orbit coupling within the Π and Δ states leads to splittings between $^2\Pi_{\frac{1}{2}}$ and $^2\Pi_{\frac{3}{2}}$, and $^2\Delta_{\frac{3}{2}}$ and $^2\Delta_{\frac{5}{2}}$, of $\gamma_1\zeta$ and $2\gamma_2\zeta$ respectively,[12] where ζ is the spin–orbit coupling of copper 3d electrons (≈800 cm^{-1}) and γ_1 and γ_2 are the orbital reduction factors for Π, Π* and Δ, Δ* excited states. This sets an upper limit of ≈1600 cm^{-1} for the splitting of a C-term pair. However, the separation of the Π and Δ states could be changed if the reduction of the orbital moment differs in different states, as it may well do.

Assignment of the ground state

The low-temperature electron paramagnetic resonance (EPR) spectrum of $[Cu_2L^{imBT}]^{3+}$ exhibits an axial set of *g* values of $g_\perp = 2.148$ and $g_\parallel = 2.002$.[13] The ground state can be assigned to $^2A_{2u}$ ($^2\Sigma^*$), on the basis of the *g* value ordering $g_\perp > g_\parallel$ and the absence of a first-order orbital moment. Spin–orbit coupling would be expected to mix a $^2A_{2u}$ ground state with ^2Eu_u (Π^*) excited states giving rise to an orbital contribution to the magnetic moment along the *X* and *Y* axes. By contrast there is no enhancement of the spin-only magnetic moment along the Cu–Cu direction, leading to $g_\parallel = g_e$ and $g_\perp > g_e$, in agreement with the results of the simulation of the EPR spectra at X- and Q-bands frequencies.[14]

Optical and MCD spectra

The optical and MCD spectra for three variants of $[Cu_2L]^{3+}$ have been reported previously by Farrar *et al.*[11] The 4.2 K absorption and MCD spectra between 25 000 cm^{-1} and 7500 cm^{-1} of $[Cu_2L^{imBT}]^{3+}$ are presented in Fig. 3(*a*) and 3(*b*) respectively. Data were collected to 5000 cm^{-1} but no additional transitions were observed. Interpretation of the electronic data is based on the view formed from earlier studies[11] that the visible and near IR spectra of these compounds are dominated by the Cu–Cu entity, the effect of the ligands being limited to the splitting of the Cu 3d atomic orbitals. For the MCD spectrum of $[Cu_2L^{imBT}]^{3+}$ presented in Fig. 3(*b*) all the observed transitions below 22 000 cm^{-1} are formally d–d transitions arising within the d-orbital manifold. Nine transitions are possible within the total d-orbital manifold to the single hole of a $[Cu_2]^{3+}$ dimer, Fig. 2(*b*). However, according to the selection rules of D_{3d} only five of these transitions are electric dipole allowed ($u \longrightarrow g$) transitions, namely a single $^2A_{2u} \longrightarrow {}^2A_{1g}$ ($\Sigma^* \longrightarrow \Sigma$) transition in the *Z* direction and four $^2A_{2u} \longrightarrow {}^2E_g$ ($\Sigma^* \longrightarrow \Pi^*$ and Δ) transitions in the *XY* plane. In addition, taking account of the orbital selection rules, $\Delta M_L = 0, \pm1$, the transitions $\Sigma^* \longrightarrow \Sigma$ and $\Sigma^* \longrightarrow \Pi^*$ will be allowed whereas $\Sigma^* \longrightarrow \Delta$ will be formally forbidden. Out of state spin–orbit coupling will relax these selection rules. A Gaussian analysis of both the absorption spectrum and MCD spectrum, to determine the position and intensity of the individual transitions, has been carried out. The fit of the MCD spectrum obtained, together with the individual Gaussian curves, is presented in Fig. 3(*c*). The data are summarised in Table 1. Nine transitions have been identified in both the absorption and MCD spectrum of $[Cu_2L^{imBT}]^{3+}$. The observation of formally forbidden transitions under D_{3d} suggests that the centre of inversion is absent, that the effective symmetry around the copper ions is lowered from D_{3d} to D_3 and that inter-state spin–orbit coupling is operative. Whilst not explicitly considered in this work, it is also possible that vibronic coupling within the excited states may result in formally forbidden transitions becoming partially allowed.

The absorption spectrum is dominated by an intense transition at 13 800 cm^{-1} (band 5). The transition moment integral for transitions from the ground state (gs) to a given excited state (es) within the $[Cu_2L^{imBT}]^{3+}$ dimer is expected to be of the form[15] shown in equation (1) where α is the coefficient of

$$\langle\psi_{es}|r|\psi_{gs}\rangle \approx (1 - \alpha^2)\langle L_{es}|r|L_{gs}\rangle + \alpha^2(R_A - R_B) \qquad (1)$$

mixing and $R_A - R_B$ is the copper–copper inter-nuclear distance. The first term represents the ligand contribution to a given transition and the second term the contribution of the two coppers A and B. Since Cu–N covalency is small, ligand contributions to the molecular orbitals are limited and the term $(1 - \alpha^2)$ in the transition moment is correspondingly small. Thus the transition moment will be dominated by the second term. Since this will be zero for transitions which do not involve bonding and anti-bonding molecular orbital combinations of the same orbital the most intense band in the absorption spectrum should be assigned to the $^2A_2 \longrightarrow {}^2A_1$ ($\Sigma^* \longrightarrow \Sigma$) transition.

The MCD spectrum is dominated by the *C*-term temperature-dependent behaviour (higher temperature data are not shown). The effects of spin–orbit coupling and a magnetic field upon the copper-based molecular orbitals can be considered by making maximum use of group theory.[16] An important general result of such analysis is that it predicts that the MCD associated with all excited states except Σ will consist of pairs of *C*-terms, opposite in sign but equal in intensity. Transitions to the $\pm\frac{1}{2}$ and $\pm\frac{3}{2}$ components of the Π and Π* excited states or the $\pm\frac{3}{2}$

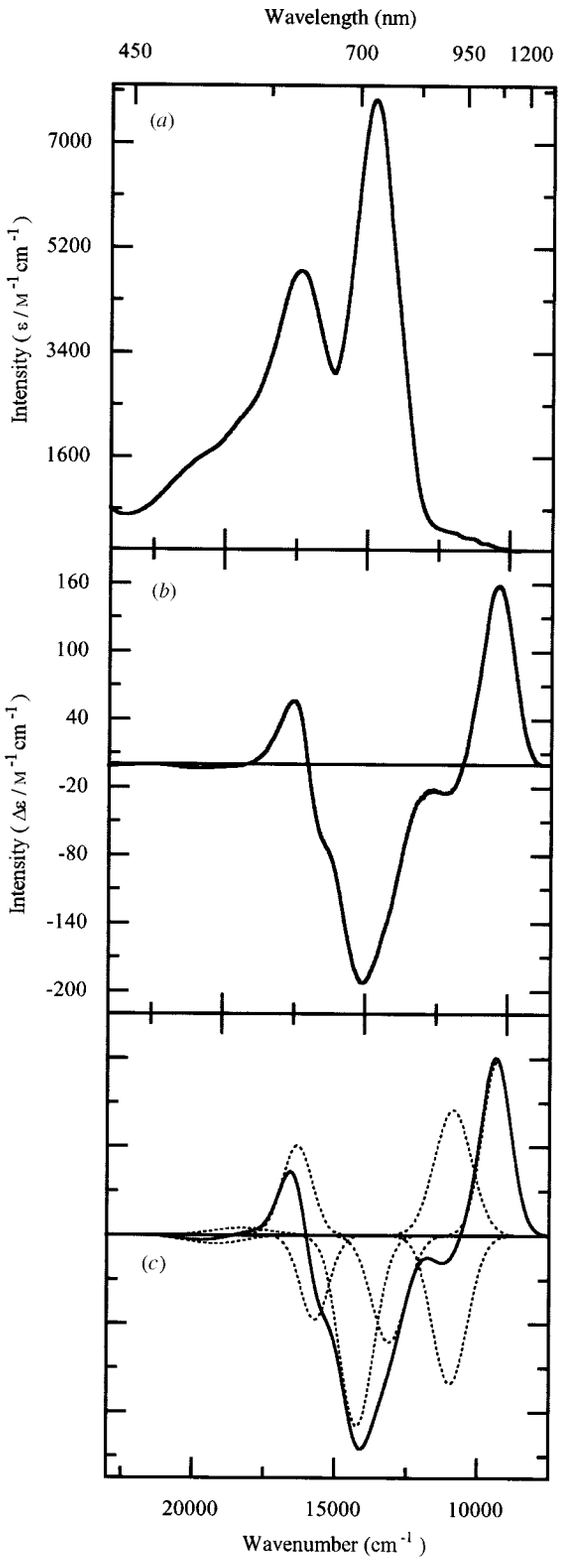

Fig. 3 (*a*) The 4.2 K absorption spectrum of $[Cu_2L^{imBT}]^{3+}$ obtained in a 1:1 (v/v) D_2O–ethane-1,2-diol solvent. (*b*) The 4.2 K MCD spectrum of $[Cu_2L^{imBT}]^{3+}$ obtained in a 1:1 (v/v) D_2O–ethane-1,2-diol solvent, (*c*) simulation of the experimental MCD data obtained as the sum of nine Gaussian curves (shown as dotted lines)

and $\pm\frac{5}{2}$ components of the Δ and Δ* excited states will exhibit positive and negative ΔA respectively. The MCD associated with the $^2A_2 \longrightarrow {}^2E$ transitions is therefore expected to consist of four pairs of oppositely signed *C*-terms as a result of spin–orbit coupling within the Π and Δ excited states. The lowest energy band of each pair is expected to be for transitions to either the $\pm\frac{1}{2}$ (Π) or $\pm\frac{3}{2}$ (Δ) component of the excited state. The $^2A_2 \longrightarrow {}^2A_1$ transition is predicted to have no MCD since the *z*-polarised transition can only gain electric dipole intensity in two orthogonal directions, which is required for significant MCD intensity, by means of spin–orbit coupling between states. In fact a small but significant C_0/D_0 ratio is found for this transition (band 5). This is an indication that the inclusion of inter-state spin–orbit coupling is important. Our calculations show that the sign of the MCD *C*-term which results from the admixture of some Π* into the Σ state is negative. Interstate spin–orbit coupling might also be responsible for the fact that the bands we have assigned to the $\Sigma^* \longrightarrow \Pi^*$ transitions (bands 6 and 7) have the negative *C*-term at lower energy, contrary to the predictions of the simple theory. However, an assessment of this problem depends sensitively upon a number of unknown quantities, in particular the splitting of the orbital energies due to the metal–metal bonding and ligand field effects. We are not yet in a position to carry out a sufficiently quantitative analysis to settle this point.

From the arguments presented above the observed MCD transitions between the Σ* ground state and the Σ, Π, Π*, Δ and Δ* excited states are assigned according to the energy level scheme in Fig. 2(*c*) and summarised in Table 1. Table 1 confirms that the pairs of bands 1/2 and 3/4 show a separation approximately twice that observed for bands 6/7 and 8/9. Thus bands 1–4 are assigned to transitions from the Σ* ground state to the Δ/Δ* excited states, whilst bands 6–9 are assigned to transitions from the Σ* ground state to Π/Π* excited states. In contrast to prediction, the lowest energy component of the Π* excited state exhibits a negative ΔA and thus has $M_J = \pm\frac{3}{2}$. The magnitude of the C_0/D_0 ratios for the $\Sigma^* \longrightarrow \Delta^*$ transitions are unexpectedly high at −12.8 and +7.6 and possibly reflect the difficulty in obtaining a reliable estimate of D_0 for such weak, broad transitions partially concealed by the intense MV $\Sigma^* \longrightarrow \Sigma$ transition.

The ordering of the orbitals in the absence of spin–orbit coupling (SOC) has been confirmed by extended Hückel molecular orbital (EHMO) calculations on a H_3N–Cu–(NH=CHCH=NH)$_3$–Cu–NH_3 model system which gave the energy level ordering of Fig. 2(*b*). The effect of SOC is shown explicitly in Fig. 2(*c*). Additionally, preliminary INDO/S calculations[15] confirm this ordering in which the ground state, under D_{3d}, is $^2A_{2u}$ (σ*), with the four δ/δ* orbitals next lowest in energy and the π/π* orbitals at lowest energy. However, such calculations under strict D_{3d} symmetry suggest a reversing of the order of the Δ and Δ* excited states such that the lowest energy pair of oppositely signed bands arise from transitions from the Δ excited states to the Σ* ground state. This possibility cannot be ruled out at the present level of interpretation.

In the experimental MCD spectra of our average-valence cryptate models[11] additional transitions are located at energies >25 000 cm^{-1}, energies which are typical for the charge-transfer transitions of aliphatic amines co-ordinated to Cu^{II} ions.[17] It may be that some of the absorption observed between 40 000 and 25 000 cm^{-1} arises from such low energy charge-transfer transitions.

Double exchange in $[Cu_2]^{3+}$ dimers

Studies of the magnetic properties of MV dimers such as iron–sulfur clusters have led to a description of the effective electronic structure in terms of model Hamiltonians which contain both Heisenberg and 'double-exchange' terms.[8,9] In the case of the $[Cu_2]^{3+}$ ion, formally a d^9d^{10} system, the Heisenberg term vanishes because one of the subunits is in a spin singlet, d^{10}, and the other in a spin doublet, d^9, state. The simplest case thus entails the consideration of only two states in which the unpaired electron can be localised on one or other side of the dimer. The energetic separation, 2*V*, between the two delocalised states is then a measure of the interaction energy, H_{AB}. Using this formalism the transition energies to be identified with 2*V* are $^2B_{3u} \longrightarrow {}^2A_g$ for Cu_A, $^2A_2 \longrightarrow {}^2A_1$ for $[Cu_2L^{imBT}]^{3+}$

Table 1 Analysis of the experimental magneto-optical data for $[Cu_2L^{imBT}]^{3+}$

Band	MCD position/cm^{-1} (relative area)	Absorption position/cm^{-1} (relative area)	Splitting/cm^{-1}	f_{osc}	C_0/D_0	Excited state[a,b]	Transition[a]
1	9 349 (0.780)	9 349 (0.003)		$1.0e^{-4}$	7.595	$^2\Delta^*_{3/2}$	
			1623				$\Sigma^* \longrightarrow \Delta^*$
2	10 972 (−0.788)	10 972 (0.002)		$1.0e^{-4}$	−12.822	$^2\Delta^*_{5/2}$	
3	10 877 (0.713)	10 877 (0.032)		$1.9e^{-3}$	0.588	$^2\Delta_{3/2}$	
			2232				$\Sigma^* \longrightarrow \Delta$
4	13 109 (−0.566)	13 109 (0.069)		$4.2e^{-3}$	−0.217	$^2\Delta_{5/2}$	
5	14 230 (−1)	13 778 (1)		$6.0e^{-2}$	−0.026	$^2\Sigma$	$\Sigma^* \longrightarrow \Sigma$
6	15 718 (−0.373)	15 978 (0.339)		$2.0e^{-2}$	−0.030	$^2\Pi^*_{3/2}$	
			625				$\Sigma^* \longrightarrow \Pi^*$
7	16 347 (0.408)	16 597 (0.370)		$2.2e^{-2}$	0.030	$^2\Pi^*_{1/2}$	
8	18 290 (0.063)	18 290 (0.275)		$1.6e^{-2}$	0.006	$^2\Pi_{1/2}$	
			924				$\Sigma^* \longrightarrow \Pi$
9	19 214 (−0.077)	19 214 (0.128)		$8.0e^{-3}$	−0.016	$^2\Pi_{3/2}$	

[a] Ground state is $^2A_2$ ($^2\Sigma^*$) in D_3 symmetry. [b] Ordering based on EHMO calculations on a H_3N–Cu–$(NH{=}CHCH{=}NH)_3$–Cu–NH_3 model.

Table 2 Effective 'double exchange' parameters for the mixed-valence copper dimers

Complex	$\|V\|$/cm^{-1}
Cu_A	4500
$[Cu_2(L^{iPrdacoS})_2]^+$	3450
$[Cu_2L^{imBT}]^{3+}$	7100

and $^2B_{2u} \longrightarrow {}^2B_{1g}$ for $[Cu_2(L^{iPrdacoS})_2]^+$. Table 2 lists the values of V for each. It should be noted that other workers have also identified the value of the double exchange parameter for Cu_A and $[Cu_2(L^{iPrdacoS})_2]^+$.[10] Whilst there is agreement in the case of $[Cu_2(L^{iPrdacoS})_2]^+$, the assignment of a different experimental band as the $\psi \longrightarrow \psi^*$ ($^2B_{3u} \longrightarrow {}^2A_g$) transition resulted in a different value of V for Cu_A.

The three examples provide an interesting comparison of the various contributions to the pathways of interaction. In the case of $[Cu_2L^{imBT}]^{3+}$, which shows the highest value of V, the interaction is dominated by $d_{z^2} - d_{z^2}$, metal–metal σ overlap since the bridging pathway, consisting of four atoms, is too long to contribute significantly. The highest occupied and lowest unoccupied molecular orbitals of the ligating nitrogen atoms are too remote in energy to contribute significantly. In the case of $[Cu_2(L^{iPrdacoS})_2]^+$ the metal–metal distance is 2.93 Å and therefore the interaction arises wholly from copper–thiolate covalency, thus emphasising the role of bridging superexchange in this case. For Cu_A, with a metal–metal distance of ≈2.5 Å and a pair of bridging thiolate ligands contributions must clearly arise from both metal–metal interactions and superexchange *via* the thiolate bridges. These conclusions are nicely confirmed by the contour plots of the ground state electron density of the three complexes. The form of the ground state orbital for each complex, obtained following INDO/S calculations,[15] is presented in Fig. 4. Comparison between the two thiolate-bridged complexes, Fig. 4(*a*) and 4(*b*), shows that for $[Cu_2(L^{iPrdacoS})_2]^+$ there is little or no direct copper–copper overlap with only the thiolate-orbitals contributing, whereas in Cu_A there are contributions from both copper d- and thiolate p-orbitals. For $[Cu_2L^{imBT}]^{3+}$, Fig. 4(*c*), ligand involvement is mainly *via* the capping nitrogen atoms lying on the Z axis. The metal–metal interaction arises almost wholly from σ overlap between the metal $3d_z^2$ orbitals directed along the metal–metal axis. This represents an example of a copper–copper bond of order 0.5 with a length of 2.38 Å.

In all cases the delocalisation energies are much higher than the likely vibronic energies, given that the values of the metal–metal vibrations in the case of the copper octaazacryptates are estimated to be a few hundred wavenumbers from the Raman spectra excited resonantly *via* the MV transition.[18] Hence the strong electronic delocalisation energy stabilises the system against valence trapping by at least an order of magnitude.

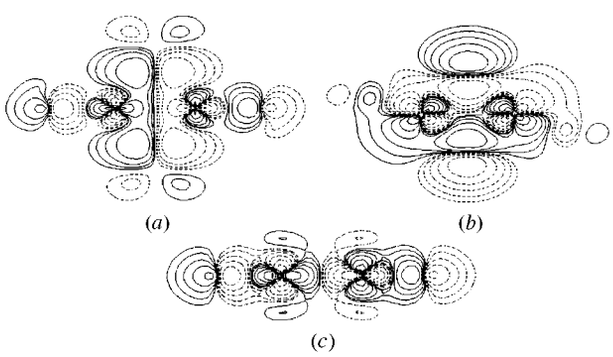

Fig. 4 Contour plots for the singly occupied MO of (*a*) the Cu_A centre found in cytochrome c oxidase and nitrous oxide reductase ($3b_{3u}$ orbital), (*b*) the $[Cu_2(L^{iPrdacoS})_2]^+$ complex ($2b_{2u}$ orbital), (*c*) the $[Cu_2L^{imBT}]^{3+}$ complex ($1a_2$ orbital). For Cu_A and $[Cu_2(L^{iPrdacoS})_2]^+$ the plane is the XY plane spanned by the two copper and sulfur atoms where the two coppers are along the X axis and the two sulfurs are along the Y axis and for $[Cu_2L^{imBT}]^{3+}$ the plane is the XZ plane, where the two coppers are along the Z axis and the X axis runs perpendicular to one of the copper–nitrogen bonds. In all cases the Cu–Cu axis is horizontal

Slight inequivalences between the copper ions can be induced without complete valence trapping when donor atoms in the metal second co-ordination sphere approach sufficiently close to one or other copper ion. This is clearly seen in the Cu_A dimer in certain chemical environments, and is reflected in a redistribution of intensity throughout the optical spectrum.[4] A complete switch to a class II valence-trapped dimer has also been observed for Cu_A by removal of one of the capping histidine residues.[19] It is clear that other forms of thiolate-bridged MV copper dimers exist in biology, notably, in the enzyme nitrous oxide reductase in a form called Cu_z which also appears to persist as a class III MV dimer.[3] Although these MV copper dimers are only now being characterised the proposal of their existence goes back to the early days of bioinorganic chemistry in the suggestion by Hemmerich[20] of their possible existence.

Experimental

Complex formation

The $[Cu_2L^{imBT}]^{3+}$ complex was prepared as described earlier.[6] The complex is soluble and stable in D_2O and the absorbance spectrum was unchanged by the addition of 50% (v/v) deuteriated ethane-1,2-diol necessary to form a low-temperature glass.

Experimental absorbance and MCD data

The absorption spectrum was recorded using a Cary17 spectrophotometer with the sample at 4.2 K in the liquid helium dewar used to measure MCD spectra. Absorption coefficient

values are quoted on the basis of the concentration determined by double integration of the EPR spectrum, recorded under non-saturating conditions, according to the method of Aasa and Vänngård.[21]

The MCD spectra were measured as previously described.[22] At low temperature the MCD spectrum is expected to be dominated by the *C*-term intensity and is thus dependent on the concentration of the paramagnetic chromophore.[16] Hence, the absorption coefficients quoted, $\Delta\varepsilon = \varepsilon_L - \varepsilon_R$ (M^{-1} cm^{-1}), refer to the concentration of the paramagnetic copper chromophore present as determined by spin integration of the copper EPR signal and are not normalised for magnetic field.

Gaussian analysis

To allow identification of the electronic transitions the absorption and MCD spectra were fitted to a sum of Gaussian curves between 22 000 cm^{-1} and 7500 cm^{-1}, using the curve fitting routine in the Origin software package (Microcal). The minimum number of curves required to fit the data satisfactorily was nine. As far as possible the position and bandwidth for each transition was kept constant whilst fitting the absorption and MCD data. As an aid to the assignment of the optical transitions the ratio of the MCD *C*-term intensity to that of the optical absorption, C_0/D_0, has been calculated. The ratio of C_0 and D_0 for each band is easily calculated from the expressions given in ref. 16 once the experimental data have been fitted to Gaussian curves. Assuming that any MCD *B*-term intensity is negligible, as will be the case at 4.2 K, then for a given band C_0/D_0 is given by equation (2), where k is the Boltzmann con-

$$\frac{C_0}{D_0} = \frac{\Delta_{MCD}}{\Delta_{ABS}} \cdot \frac{\Delta\varepsilon_{calc}}{\varepsilon_{calc}} \cdot \frac{\nu_{ABS}}{\nu_{MCD}} \cdot \frac{kT}{\mu_B \cdot B} \qquad (2)$$

stant, T is the absolute temperature, μ_B is the Bohr magneton ($\approx 9.274 \times 10^{-24}$ J T^{-1}) and B is the magnetic field strength at which the MCD spectrum is measured. The values of Δ, ν, $\Delta\varepsilon_{calc}$, and ε_{calc} are those obtained from the Gaussian analysis. Thus 2Δ is the full width at half maximum height, ν_{ABS} and ν_{MCD} are the calculated energies of the band maxima for the absorbance and MCD spectra respectively, ε_{calc} is the band height at ν_{abs} for the absorption spectrum and $\Delta\varepsilon_{calc}$ is the band height at ν_{MCD}. The value of $\Delta\varepsilon_{calc}$ used in the above expression is increased by a factor of 1.25 compared to the value obtained from the Gaussian analysis to account for the non-linearity of the MCD signal at 4.2 K and 5 T due to the onset of magnetisation (saturation), as expected for a $S = \frac{1}{2}$ system, due to the Boltzmann effect.

The oscillator strength, f_{osc} ($= 4.32\ e^{-9} \times$ area of the curve), for each absorbance band has also been calculated.[16]

EHMO calculations

The energy level scheme of Fig. 2(*b*) has been derived using an extended Hückel molecular orbital (EHMO) approximation[23] using the parameters in Table 3. The H_{ij} values have been calculated by means of a modified Wolfsberg–Helmholtz approximation.[24] The basis molecule was chosen as H_3N–Cu–$(NH{=}CHCH{=}NH)_3$–Cu–NH_3, which effectively represents the complex of interest, $[Cu_2L^{imBT}]^{3+}$, whilst preserving the essential symmetry elements and keeping the number of atoms to a reasonable size. The atomic orbitals included in the calculation were the H 1s, C 2s and 2p, N 2s and 2p and Cu 4s, 4p and 3d. The point group is D_{3d} if only the first co-ordination sphere of the copper is taken into account.

INDO/S calculations

The ROHF-INDO/S (intermediate neglect of differential overlap/spectroscopic parameterisation) calculations are described in detail elsewhere.[15] For the contour plots presented in Fig. 4 the orbitals were evaluated on a 65 × 65 point grid in a suitable molecular plane of dimension 10 × 10 Å. Contours were drawn at values of $\psi = \pm 0.005$, ± 0.01, ± 0.020, ± 0.040 (e $Å^{-3})^{\frac{1}{2}}$. All plots show the singly occupied MO in the corresponding molecule.

Table 3 Parameters used in the EHMO calculations

Orbital	H_{ii}/eV[a]	ζ_1
Cu 3d	−14.00	5.95[b]
Cu 4s	−11.40	2.20
Cu 4p	−6.06	2.20
N 2p	−13.40	1.95
N 2s	−26.00	1.95
C 2p	−11.40	1.63
C 2s	−21.40	1.63
H 1s	−13.60	1.30

[a] eV ≈ 1.602×10^{-19} J. [b] $\zeta_2 = 2.30$, $c_1 = 0.5933$, $c_2 = 0.5744$.

Acknowledgements

Financial support from the BBSRC/EPSRC *via* the funding of the Centre for Metalloprotein Spectroscopy and Biology (to A. J. T. and J. A. F.), from the European Union *via* the MASIMO program (to A. J. T., J. A. F. and F. N.) and from the Deutsche Forschungsgemeinschaft (to F. N.) is gratefully acknowledged.

References

1 M. B. Robin and P. Day, *Adv. Inorg. Chem. Radiochem.*, 1967, **10**, 247.
2 P. M. H. Kroneck, W. E. Antholine, J. Riester and W. G. Zumft, *FEBS Lett.*, 1988, **242**, 70.
3 J. A. Farrar, A. J. Thomson, M. R. Cheesman, D. M. Dooley and W. G. Zumft, *FEBS Lett.*, 1991, **294**, 11.
4 J. A. Farrar, F. Neese, P. Lappalainen, P. M. H. Kroneck, M. Saraste, W. G. Zumft and A. J. Thomson, *J. Am. Chem. Soc.*, 1996, **118**, 11 501.
5 R. P. Houser, V. G. Young, jun. and W. B. Tolman, *J. Am. Chem. Soc.*, 1996, **118**, 2101.
6 C. Harding, V. McKee and J. Nelson, *J. Am. Chem. Soc.*, 1991, **113**, 9684.
7 M. E. Barr, P. H. Smith, W. E. Antholine and B. Spencer, *J. Chem. Soc., Chem. Commun.*, 1993, 1649.
8 G. Blondin, S. Borshch and J. J. Girerd, *Comments Inorg. Chem.*, 1992, **12**, 315.
9 G. Blondin and J. J. Girerd, *Chem. Rev.*, 1990, **90**, 1359.
10 K. R. Williams, D. R. Gamelin, L. B. LaCroix, R. P. Houser, W. B. Tolman, T. C. Mulder, S. de Vries, B. Hedman, K. O. Hodgson and E. I. Solomon, *J. Am. Chem. Soc.*, 1997, **119**, 613.
11 J. A. Farrar, V. McKee, A. H. R. Al-Obaidi, J. J. McGarvey, J. Nelson and A. J. Thomson, *Inorg. Chem.*, 1995, **34**, 1302.
12 See for example, Chapter 5, eqn. 5.8 in G. Herzberg, *Molecular Spectra and Molecular Structure. I. Spectra of Diatomic Molecules*, Van Nostrand, New York, 1950.
13 C. Harding, J. Nelson, M. C. R. Symons and J. Wyatt, *J. Chem. Soc., Chem. Commun.*, 1994, 2499.
14 F. Neese, Diplomarbeit, Universität Konstanz, 1993.
15 F. Neese, Ph.D. Thesis, Universität Konstanz, 1996.
16 S. B. Piepho and P. N. Schatz, *Group Theory in Spectroscopy with Applications to Magnetic Circular Dichroism*, Wiley-Interscience, New York, 1983.
17 A. B. P. Lever, *Inorganic Electronic Spectroscopy*, Elsevier, Amsterdam, 1983, p. 554 ff.
18 A. H. R. Al-Obaidi, G. Baranovich, J. Coyle, C. Coates, J. J. McGarvey, V. McKee and J. Nelson, unpublished work.
19 J. A. Farrar, P. Lappalainen, W. G. Zumft, M. Saraste and A. J. Thomson, *Eur. J. Biochem.*, 1995, **232**, 294.
20 P. Hemmerich, in *The Biochemistry of Copper*, eds. J. Peisach, P. Aisen and W. E. Blumberg, Academic Press, New York, 1966, pp. 5–34, 269–270.
21 R. Aasa and T. Vänngård, *J. Magn. Reson.*, 1975, **19**, 308.
22 A. J. Thomson, M. R. Cheeseman and S. J. George, *Methods Enzymol.*, 1993, **226**, 199.
23 R. Hoffmann, *J. Chem. Phys.*, 1963, **39**, 1397.
24 J. H. Ammeter, H. B. Bürgi, J. C. Thibeault and R. Hoffmann, *J. Am. Chem. Soc.*, 1978, **100**, 3686.

Received 23*rd June* 1997; *Paper* 7/04392I